Available online www.ejaet.com

European Journal of Advances in Engineering and Technology, 2022, 9(11):29-42

Research Article ISSN: 2394 - 658X

Development and Simulation of Kinematic and Dynamic Models of a Mobile Robot with Embedded Arm

Oswald Jordane Nneme* and Jean Mbihi

Laboratory of Computer Science Engineering and Automation, University of Douala,
P. O. Box 1872 Douala, Cameroon
*Corresponding author: oswaldnneme@gmail.com

ABSTRACT

This paper deals with of a 2WD Mobile robot with embedded 4DOF arm, involving sequences of chassis motion on the floor and target spatial paths of the arm. The kinematic equations of the 2WD mobile chassis are developed from a geometric analysis approach, and the kinematic model of the robotic arm is obtained in the chassis frame using Denavid Hardenberg method. Then, the dynamic models of both mobile chassis and robotic arm result from decoupling approaches. Furthermore, the corresponding kinematic and dynamic virtual schemes are implemented within Matlab/Simulink platform. Finally, the virtual simulation results obtained for a variety of operating modes and conditions, show the high quality of the proposed decentralized kinetic and dynamic models for 2WD mobile robots with 4DOF arm.

Key words: Mobile robot, robotic arm, kinematic and dynamic models, virtual simulation schemes

---

INTRODUCTION

Modern robots are dedicated machines, involving fixed and mobile parts for repetitive works, associated with "smart" control devices. Therefore, they are designed and built for partially or totally replacing human experts for executing various physical tasks in numerous application fields, e.g. Civil manufacturing factory [1]-[2], load lifting or shifting [3], devices detection or inspection for prevention [4], underwater navigation [5]-[6], military applications [7], social and home automation [8]-[9], surface painting [10]-[11], medical surgery [12]-[12], sewing and embroidering of special textile materials [13]-[14], even children toys [15]-[16], and education laboratory [17]. In all these cases, position and even speed tracking strategies, are relevant technical requirements.

Obviously, because of the need to rigorously meet operation needs and constraints of so many application areas of robots, modern robots involve many building morphologies. However, most popular robots consist of *n*DOFA (*n* Degree Of Freedom Arm), *m*WDC (*m* Wheel Drive Chassis), or a combined *m*WDC-*n*DOFA morphology. For these popular robotic morphologies, $m \in \{2, 4\}$ and $n \in \{1, 2, 3, 4, 5, 6\}$.

In modern robotic engineering, abundant published papers are encountered on the modelling and control of *m*WDC mobile robots [18]-[21], and *n*DOFA robots [22]-[24]. However, a few published works are encountered on the combined *m*WDC-*n*DOFA robotic morphology [25]-[26].

In this paper, a combined *2*WDC-*4*DOF robotic morphology is considered as shown in Fig. 1. Then, the target goal is to study the kinematic and dynamic models as well as corresponding virtual schemes of both parts, with validation by virtual simulation tests. The remaining sections of the paper are organized as follows: Kinematic and Dynamic study of the *2*WDC mobile robot, Kinematic and Dynamic study of *4*DOFA robot, combined Kinematic and Dynamic of the Combined *2*WDC-*4*DOF robotic system, virtual simulation results, conclusion and references.

KINEMATIC AND DYNAMIC STUDY OF 2WDC-4DOFA ROBOT

A mobile manipulator consists of a mobile base and a manipulator [27], which represents several advantages and various constraints [28]. The most important feature of a mobile manipulator is the flexible operational workspace in contrast with the limited workspace of a fixed manipulator. This feature endows a mobile manipulator with the ability to operate in a large scale of operation [29], such as handling and transporting parts from one place to another. Moving mobile manipulators systems, present many unique problems that are due to the coupling of holonomic manipulators with nonholonomic bases.

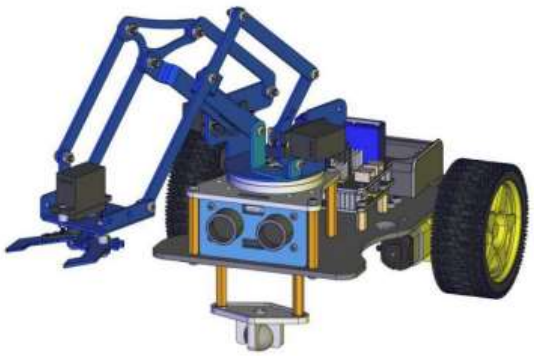

Fig. 1 2WD Mobile robot with embedded 4DOF arm [27]

Kinematic model and Simulink Scheme of 2WDC mobile robot

In the study of kinematics, only the speeds are taken into account. The motion of a mobile robot with differential drive is characterized by two kinematic constraints, namely:

- No lateral slide,
- Unsliding turning.

Let $\{X_I, Y_I\}$ be any fixed reference frame and $\{X_r, Y_r\}$ a moving frame of reference related to the robot. Let $q^i = [x^i, y^i, \theta^i]^T$ be a point of the frame $\{X_I, Y_I\}$ and $q^r = [x^r, y^r, \theta^r]$ a point of the frame $\{X_r, Y_r\}$. The points q^i and q^r are related by the orthogonal matrix $R(\theta)$.

$$q^i = R(\theta)\, q^r \quad \text{with} \quad R(\theta) = \begin{pmatrix} cos\theta & -sin\theta & 0 \\ sin\theta & cos\theta & 0 \\ 0 & 0 & 1 \end{pmatrix} \tag{1}$$

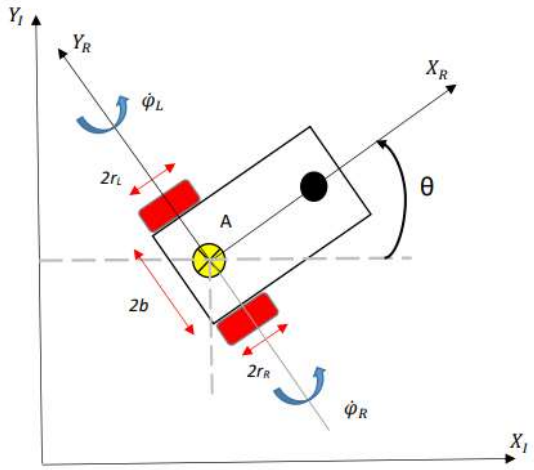

Fig. 2 Aerial view of the mobile base

Fig. 2 shows the unicycle-type mobile robot in the fixed and mobile frames.
A : is the midpoint of the wheel axis.
$2r_L$: is the diameter of the left wheel of the robot;
$2r_R$: is the diameter of the right wheel of the robot;
2b : is the width of the robot;

$\dot{\varphi}_r$ *et* $\dot{\varphi}_l$: represent respectively the rotation speed of the right wheel and the left wheel;
θ : is the orientation angle of the robot;
The objective is to move the mobile robot (q^r) to a precise position defined by the fixed reference frame $\{X_I, Y_I\}$ by determining the control parameters *v* and *ω*. In the mobile reference frame $\{X_r, Y_r\}$ the coordinates of the point q^r are: (2)

$$\begin{cases} \dot{x}^r = v \\ \dot{y}^r = 0 \\ \dot{\theta}^r = \omega \end{cases}$$

Using equation (1), we can write

$$\begin{pmatrix} \dot{x}^i \\ \dot{y}^i \\ \dot{\theta}^i \end{pmatrix} = \begin{pmatrix} cos\theta & -sin\theta & 0 \\ sin\theta & cos\theta & 0 \\ 0 & 0 & 1 \end{pmatrix} \begin{pmatrix} \dot{x}^r \\ \dot{y}^r \\ \dot{\theta}^r \end{pmatrix} \quad (3)$$

Direct Kinematic

The expression for the linear velocity *v* and the angular velocity *ω* of the mobile robot are obtained as a function of the rotational speeds of the left wheel $\dot{\varphi}_l$ and the right wheel $\dot{\varphi}_R$.In Fig. 3 we can see the direct kinematic block under Simulink. (4)

$$\begin{cases} v = \dfrac{R(\dot{\varphi}_R + \dot{\varphi}_L)}{2} \\ \omega = \dfrac{R(\dot{\varphi}_R - \dot{\varphi}_L)}{2L} \end{cases}$$

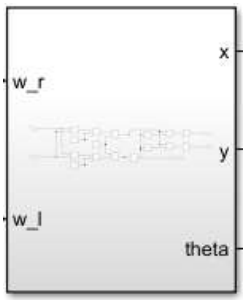

Fig. 3 2WD Direct kinematic block

Inverse kinematic

The reverse kinematic model eq. (5), is computed using eq. (4).In Fig 4 we can see the inverse kinematic block under Simulink.

$$\begin{cases} \dot{\varphi}_R = \dfrac{v + L\omega}{R} \\ \dot{\varphi}_L = \dfrac{v - L\omega}{R} \end{cases} \quad (5)$$

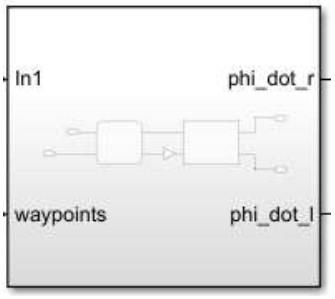

Fig. 4 2WD Inverse kinematic bloc

Dynamic model and Simulink Scheme of 2WDC robot

Model identification is achieved using a simple and inexpensive data acquisition system. An Arduino Uno embedded board system is used to collect sensor data, send it to the computer, and control the model. Data processing is performed using MATLAB/SIMULINK.

The dynamic system used in this paper is a two-wheel drive mobile robot with two independent DC servo mechanisms equipped with a manipulator arm, as shown in Figure 1. Due to the unavailability of the dynamic model associated with the 2WD robot with manipulator arm, it will be developed using the experimental modeling approach, i.e., based on real data acquired during tests and measurements [31]. Since the 2WD robot consists of 02 equivalent servomechanisms (e.g., one servomotor with one gear for each case), the following assumptions are used to develop a complete dynamic decoupling model.

- The two servo mechanisms have identical electrical/mechanical characteristics;
- Both gearmotors are subjected to rotational and load constraints during robot motion;
- The experimental modeling error can be rigorously cancelled under conditions by a robust controller.

In addition, the experimental models of the two servomechanisms are similar, while the logistic materials used to obtain the experimental data are given as follows:

- 02 similar servomechanisms (DC motor with gear) ;
- 02 optical encoders, each for a single servomechanism;
- 02 encoder disks with 20 slots, each for a single servomechanism;
- Arduino Uno microcontroller;
- Lithium-polymer battery 8,4 V.

Markov Djoumessi Mbihi[21] in his article on the optimal control of a mobile robot, was able to define a dynamic model that is based on an experimental principle. In our case the chassis of the mobile robot has an arm. In Fig. 5 we can observe the dynamic block of the mobile base system under Simulink.

$$G(s)_{EOL} = \frac{41.83}{s^2+8.699s+12.91}$$
$$G(s)_{EOL} = \frac{K_s\omega_n^2}{s^2 + 2\xi\omega_n s + \omega_n^2} \quad (6)$$

With

$$K_s = \frac{41.83}{12.91}; \omega_n = \sqrt{12.91}; \xi = \frac{8.699}{2\omega_n}$$

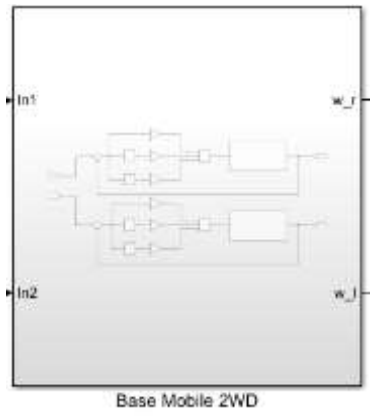

Fig. 5 2WD dynamic block

Kinematic model and Simulink Scheme of the 4DOFA robot

Robotic kinematics studies the motion of a robotic mechanism independently of the forces and torques that cause it. It allows to calculate the position and orientation of the robot manipulator's end effector with respect to the manipulator's base according to the joint variables as shown in Fig. 6. Robotic kinematics is fundamental to the design and control of a robotic system. In order to deal with the complex geometry of a robot manipulator, properly chosen coordinate markers are attached to various parts of the mechanism. Manipulator kinematics primarily studies how the locations of these frames change as the robot joints move. Kinematics focuses on position, velocity and acceleration, and an accurate kinematic model must be established to study the motion of a robot manipulator.

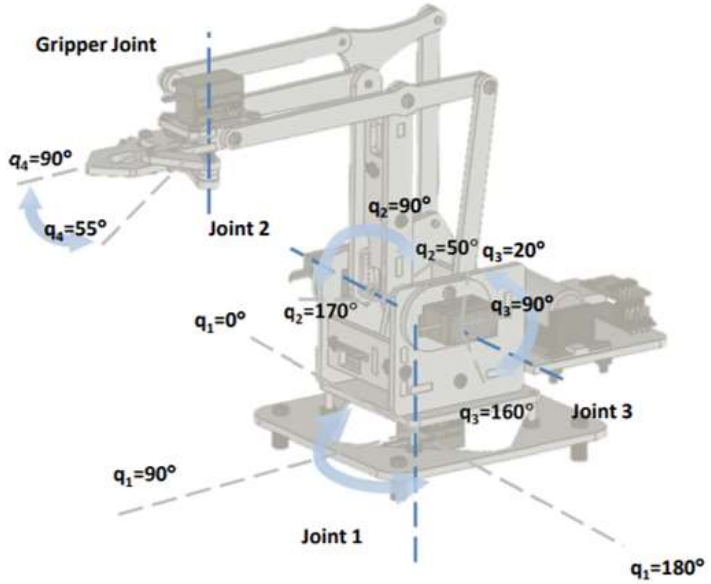

Fig. 6 Position of the different joints [30]

Direct kinematic

Direct kinematics refers to the use of a robot's kinematic equations to calculate the end effector position from specified values. To implement linear control, we need to calculate the position of the gripper from the joint angles. The distance of the wrist from the axis of joint 1 is calculated as follows:

$$r = -l_2 cos\theta_2 - l_3 cos(\theta_2 + \theta_{3,0}) \tag{7}$$

On the other hand, the height of the clamp is calculated from:

$$p_{T,z} = h_1 + l_2 sin\theta_2 + l_3 sin(\theta_2 + \theta_{3,0}) \tag{8}$$

The x and y coordinates of the clamp are:

$$p_{T,x} = l_0 + (r + l_1 + l_5) sin\theta_1 - d_5 cos\theta_1$$
$$p_{T,y} = -(r + l_1 + l_5) cos\theta_1 - d_5 sin\theta_1 \tag{9}$$

In Fig. 7 we can see the direct kinematic block of the manipulator under Simulink.

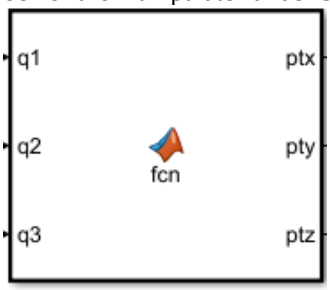

Fig. 7 Arm Direct kinematic bloc**k**

Inverse kinematic

If the poses are given in Cartesian space, then we must use inverse kinematics to calculate the joint configurations. The calculation will be performed in three steps:

1. The joint θ_1 is calculated from the x and y coordinates of the end-member as shown in Fig. 8. Due to the non-zero term d_5, the calculation of θ_1 must be obtained from the sum of two angles. The point of the clamp wrist relative to the robot p_W^0, can be calculated as follows:

$$\theta_1 = arctan\left(\frac{p_{T,x} - l_0}{-p_{T,y}}\right) + arcsin\left(\frac{d_5}{\sqrt{(p_{T,x} - l_0)^2 - p_{T,y}^2}}\right) \tag{10}$$

$$p_W^0 = p_T + \begin{bmatrix} l_5 sin\theta_1 - l_0 \\ -l_5 cos\theta_1 \\ 0 \end{bmatrix}$$

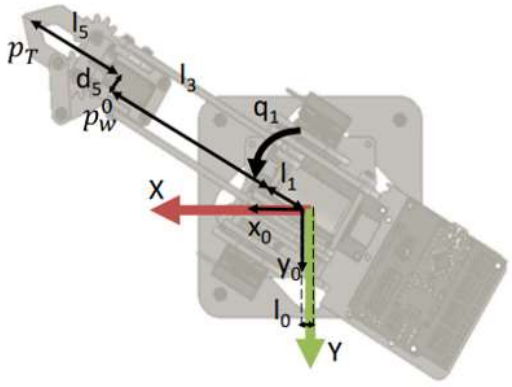

Fig. 8 Aerial view of the manipulator [30]

2. The coordinates of the joints θ_2 and $\theta_{3,0}$ are calculated from the triangle formed by links 2 and 3 of a conventional robot arm :

$$\begin{gathered} r = \sqrt{p_{w,x}^2 + p_{w,y}^2} - 1 \\ z_e = p_{w,z} - h_1 \\ \alpha = arctan\left(\frac{z_e}{r}\right) \\ s = \sqrt{r^2 + z_e^2} \\ \gamma = arccos\left(\frac{l_2^2 + l_3^2 - s^2}{2l_2 l_3}\right) \\ \beta = arccos\left(\frac{s^2 + l_2^2 - l_3^2}{2sl_2}\right) \\ \theta_{3,0} = \pi - \gamma \\ \theta_2 = \pi - \alpha - \beta \end{gathered} \tag{11}$$

3. Finally, the angle of the third joint θ_3 is calculated from the inverse kinematics of the four-bar mechanism as shown in Fig. 9:

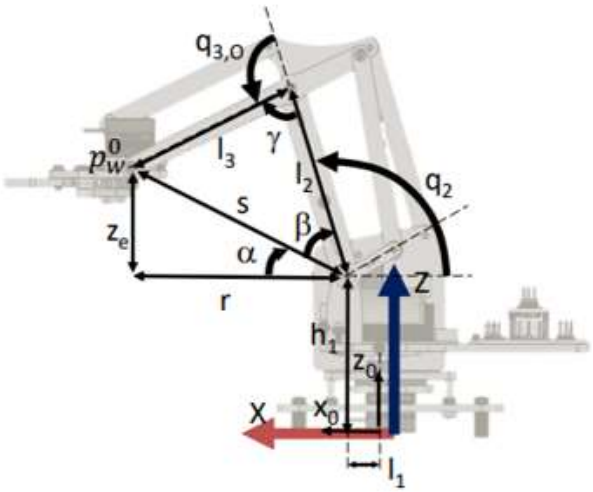

Fig. 9 Inverse kinematic mechanism [30]

$$e = \sqrt{l_{3,0}^2 + l_2^2 - 2l_{3,0}l_2 cos\theta_{3,0}} \tag{12}$$

$$\rho = arcsin\left(\frac{l_{3,0} sin\theta_{3,0}}{e}\right)$$

$$\varphi = arccos\left(\frac{e^2 + l_{3,I}^2 - l_4^2}{2el_{3,I}}\right)$$

$$\theta_3 = \rho + \varphi + \frac{\pi}{2} - \theta_2$$

There are several configurations (solutions) that can achieve the desired installation. However, due to mechanical constraints, there is only one possible configuration. In Fig. 10 we can see the inverse kinematic block of the manipulator under Simulink.

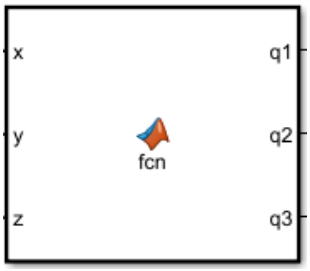

Fig. 10 Arm Inverse kinematic bloc

Dynamic model and Simulink Scheme of the 4DOFA robot

According to the research of LOGA [22] we used his method of modelling servomechanisms with delay. From the step response on an isolated real servo mechanism, the "System Identification" tool in MATLAB 2018a software is used to obtain the shape of the behavior and the corresponding open-loop transfer function [32]. The transfer function, characteristic of servomechanisms, thus deduced is:

$$G_{\theta j} = K\frac{e^{\lambda_j s}}{(1+\tau_j s)(1+\tau_j' s)} \tag{13}$$

We can observe that servomechanisms can be dissociated into two first order systems [30]. This system has two poles as shown in equation:

$$\begin{cases} x_1 = -\dfrac{1}{T_1} \\ x_2 = -\dfrac{1}{T_2} \end{cases} \tag{14}$$

Comparing the real parts,, x_2 is the dominant pole with time constant T_2 as presented in equation (14) :

$$|R(x_1)| < |R(x_2)| \tag{15}$$

The open-loop transfer function of the real SISO servomechanism is represented by the equation:

$$G_{\theta j} = K\frac{e^{\lambda_j s}}{(1+\tau_j' s)} \tag{16}$$

with τ'=T_2. The index j is the variable of the SISO mechanisms available in the robotic chain [26].

- Static gain K = K1 = K2 = K3 =0.001;
- Time constant τ'=τ1 = τ"2 = τ"3 =0.0271 s;
- Time delay λ=λ1 = λ2 = λ3 = 0.0128 s.

In Fig. 11 we can observe the dynamic block of the manipulator system under Simulink.

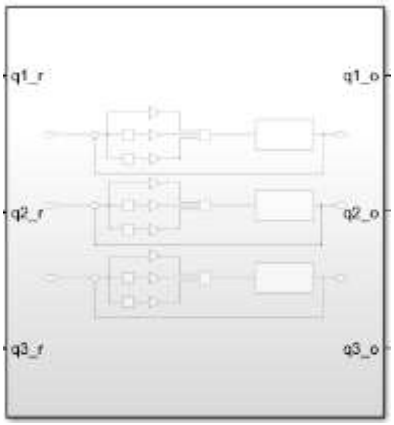

Fig. 11 Arm Dynamic block

Combined Simulink kinematic and dynamic Schemes of 2WDC-*4*DOFA robot

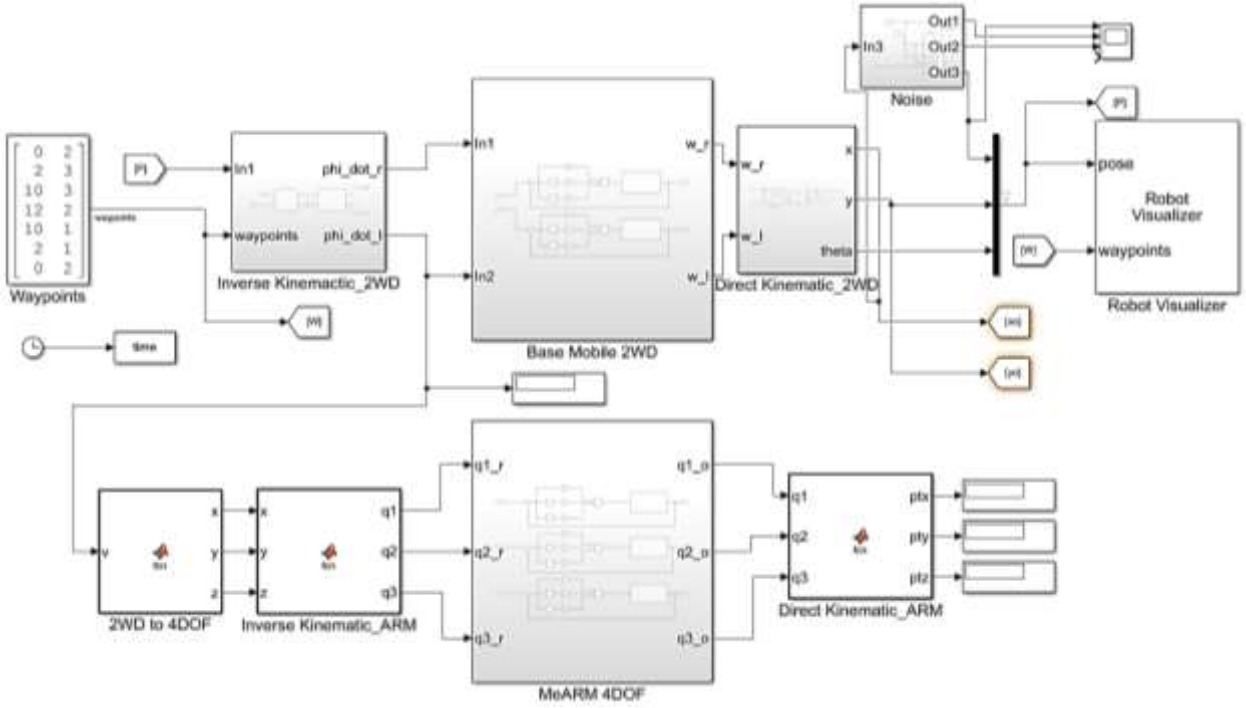

Fig. 12 2WD Mobile robot with embedded 4DOF arm on Simulink

Our simulation allows us to control the base and the manipulator sequentially. The manipulator will perform its trajectory tracking only when the base has reached its target and the wheel speed goes to 0. We want to ensure that the arm performs its movement when the base is stationary.

The first part is the prototyping of the mobile base as shown in Fig. 12. We can see an inverse kinematic control block, a dynamic control block and then a direct kinematic block. The equations seen in the chapter on Kinematic model and Simulink Scheme of 2WDC mobile robot allowed us to perform the different blocks in Simulink. As soon as the Mobile base reaches the target, the speed at the wheels (phidotR and phidotL) goes to 0.

The second part concerns the prototyping of the manipulator arm. We can observe the presence of an inverse kinematics block, a dynamic control block and a direct kinematics block. The equations seen in chapter concerning the control strategy of the manipulator arm allowed us to carry out the different blocks under Simulink.

There is a transition part between the base and the arm parts. We define a matlab function, which will change the setpoint according to the wheel speeds. That is to say as long as the speed of the wheels is different from 0 it would mean that the base is in movement and therefore the arm must remain fixed at its initial position. Now when the speed goes to 0 it means that the mobile base is immobile. At this moment the set point at the arm level changes and the manipulator can carry out its trajectory tracking. The transition between the base and the arm is done thanks to the speeds of the wheels of the base.

RESULTS AND DISCUSSIONS

Parameterization

When we run a simulation in Simulink it is necessary to define some parameters. First the simulation parameters are shown in Table 1.

Table -1 Robot simulation condition

Robot Simulation Condition	
Sampling time	0,0001 s
Types of numerical solvers	Ode45

The parameters in Table 2 are the exact configurations of the robot seen in Fig. 1 and Fig. 8.

Table -2 Robot Configuration

Mobile Base	
Radius of a wheel (R)	0,0095 m
Distance between two wheels (2b)	0.48 m
Manipulator arm	
L0	5 mm
L1	15.1 mm
L2	80 mm
L3	80 mm
L3I	23.9 mm
L3O	35 mm
L4	80 mm
D5	10.7 mm

Trajectory

Our trajectory is defined by point positions in the reference frame (x, y, z) as shown in Table 3.

Table -3 Robot Pose

Pose of the base	
x	[0 ;2 ;10 ;12 ;10 ;2 ;0] m
y	[0 ;3 ;3 ;2 ;1 ;1 ;2] m
Pose of the manipulateur	
x	[100 ;80 ;20] mm
y	[50 ;70 ;100] mm
z	[100 ;20 ;50] mm

The simulation results are obtained without disturbance. While the robot is moving, we have visualized the behavior of the wheels. We observe that the wheels of the robot follow the set point with precision as shown in Fig. 13 and 14. From 90s the set point goes to 0.

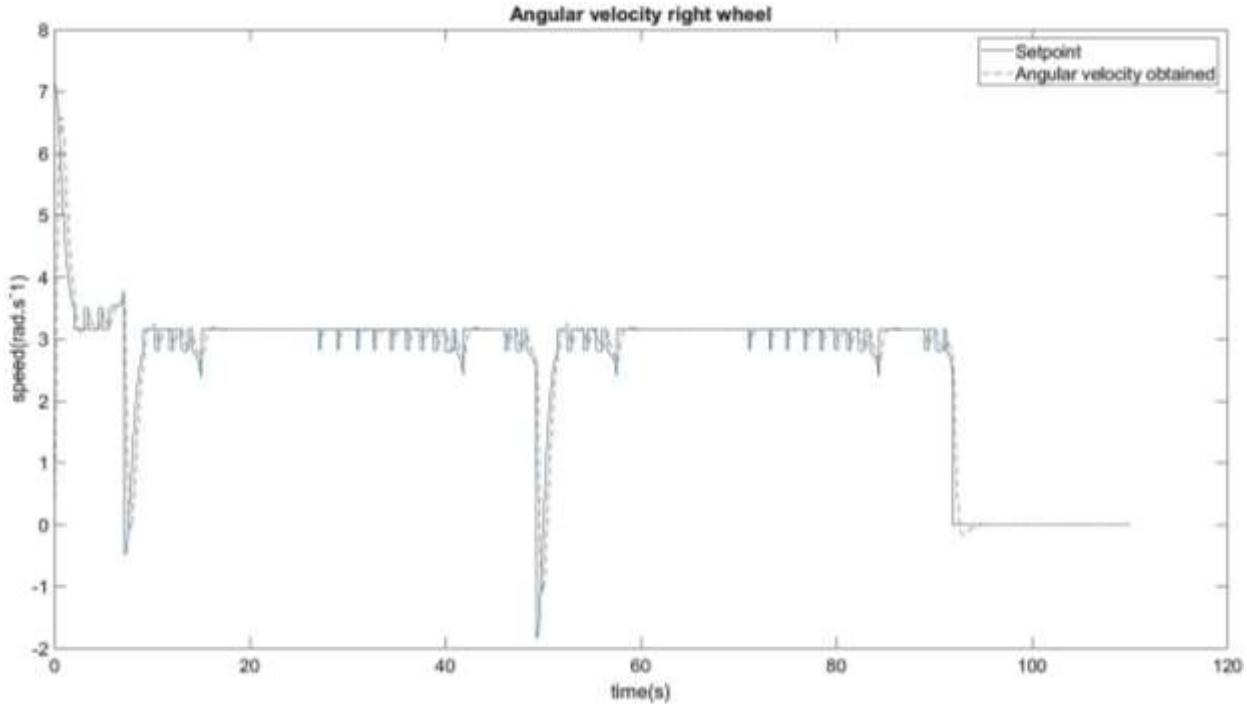

Fig. 13 Angular velocity right wheel

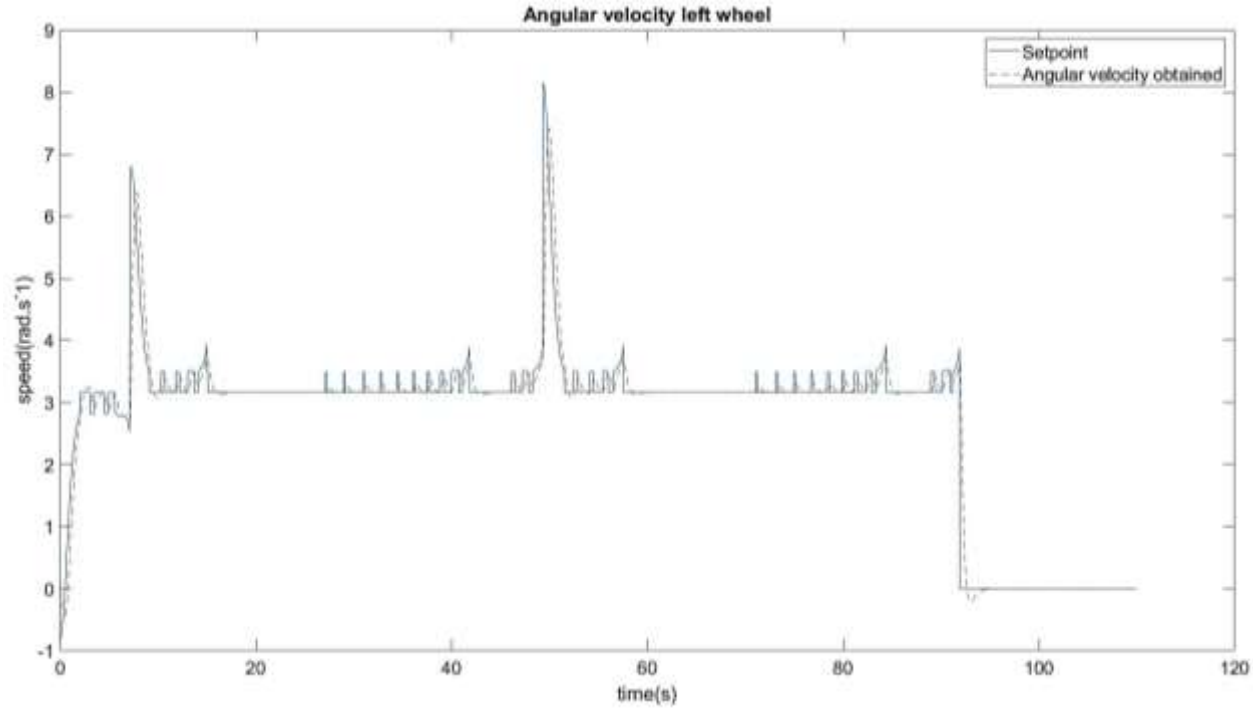

Fig. 14 Angular velocity left wheel

When the mobile base moves, the manipulator arm keeps its initial position during all the travel of the mobile base as shown in Fig. 15, 16 and 17. As soon as the mobile base is static (objective reached), the manipulator changes its position.

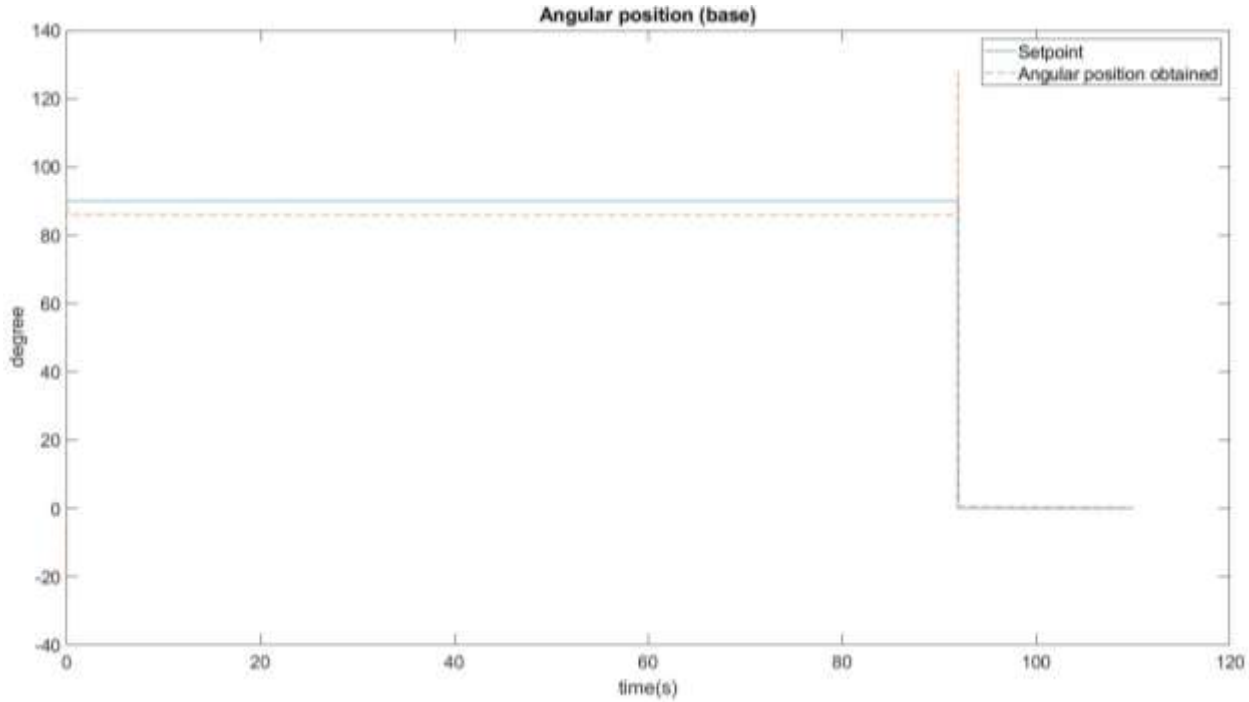

Fig. 15 Angular position (base)

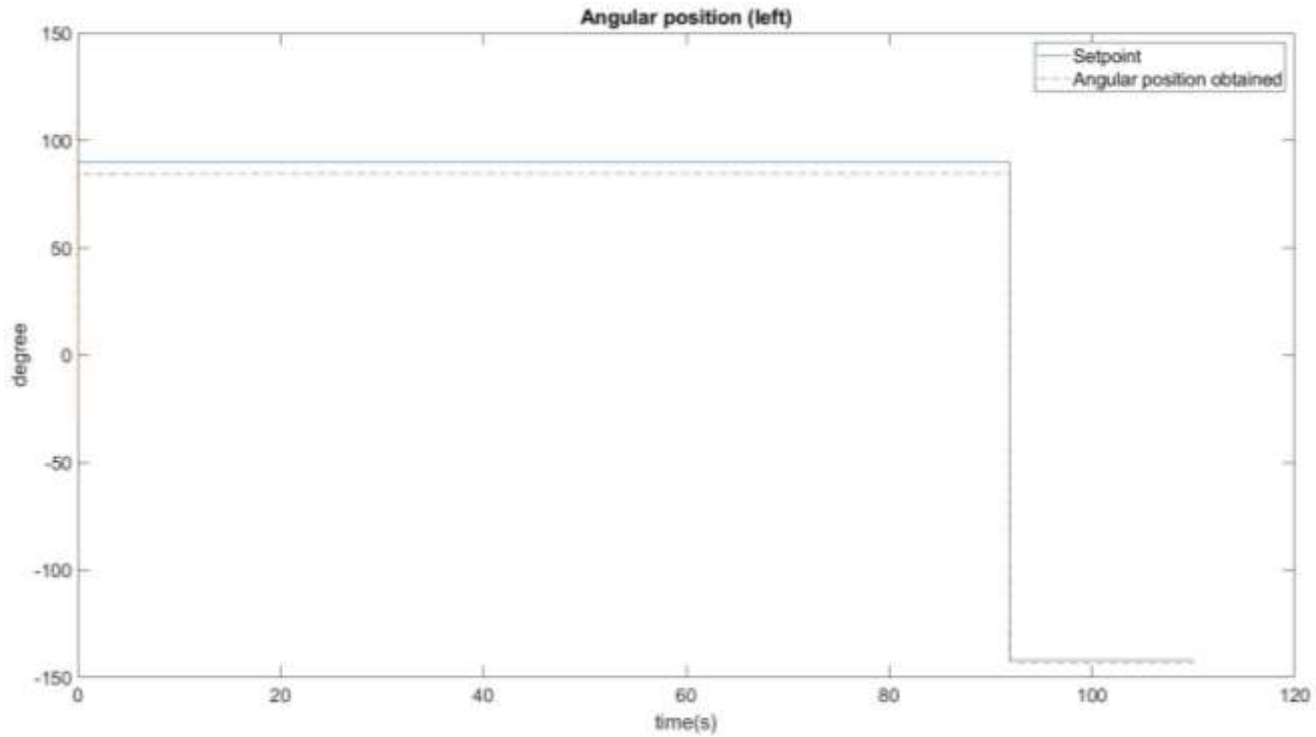

Fig. 16 Angular position (left)

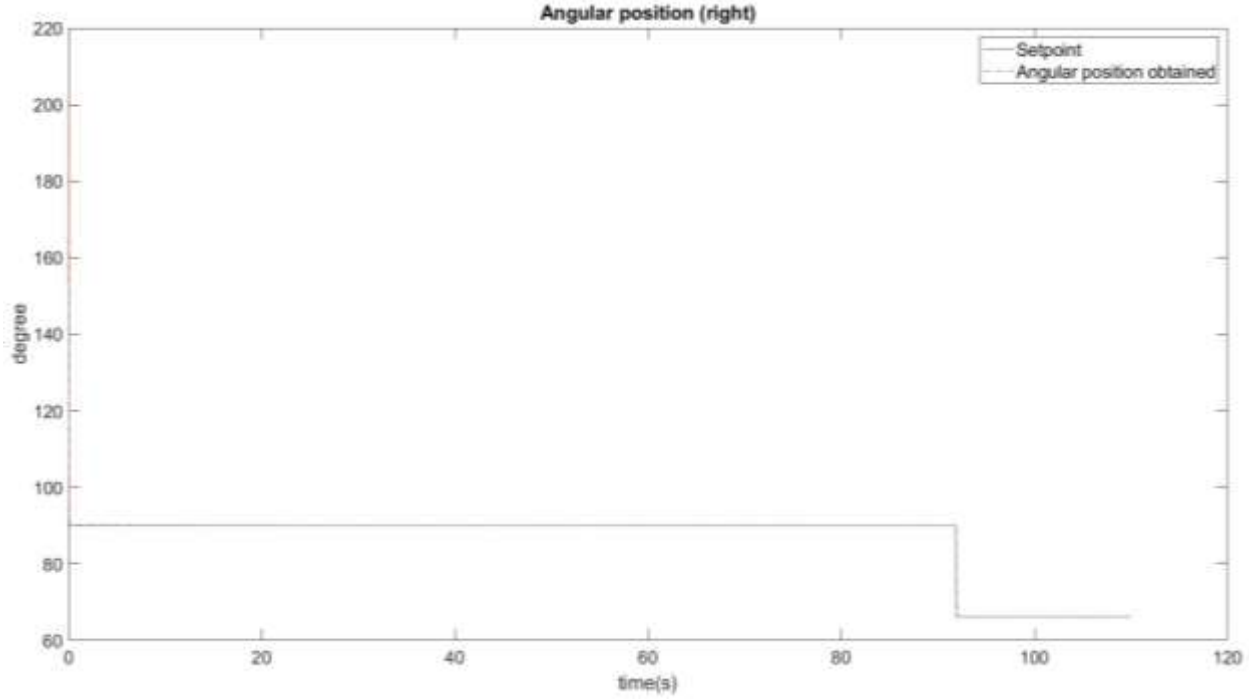

Fig. 17 Angular position (right)

We can observe that the algorithm allows a change between the mobile base and the arm in an efficient way. The mobile base reaches the target at 95s and at the same time the right and left wheels receive an angular velocity of zero. At the same minute the manipulator arm changes its target since the mobile base is stationary. Now what happens when the mobile base is disturbed before and after reaching its objective?

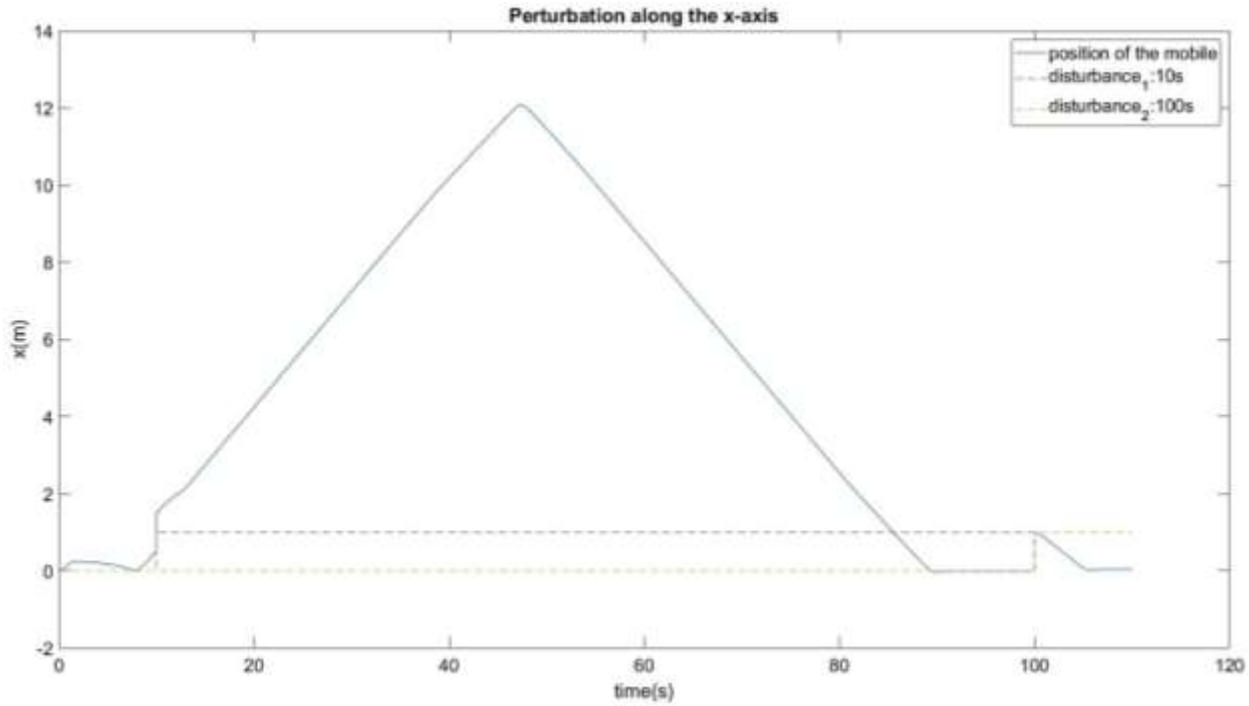

Fig. 18 Disturbance along the x-axis

The perturbations will be performed exclusively on the mobile base. These perturbations will be similar to a push of the hand on the mobile base along the x-axis. It will be an external perturbation. We have added two step inputs to

simulate a push as shown in Fig. 18. The first step will be triggered at 10s while the mobile base is moving while the second step will be triggered at 100s when the mobile base is stationary. Both steps have a step value of 1, which is equivalent to a thrust of 1 meter.

CONCLUSION

We can observe that the algorithm of switching mobile base and manipulator works. The base carries out its trajectory until reaching the final objective during this time the arm remains motionless. Around 58 seconds the mobile base has reached the final objective and the angular speed of the wheels converges to 0. This would simply mean that the mobile is immobile. The braking system of the mobile base is established by a servo-control of the wheels having 0 as set point (Absence of rotation). As soon as the base is immobile, we can observe an activity at the level of the manipulator arm. Fig. 18 and 19 allowed us to observe a failure in the regulation. It is necessary to look at a much more robust and optimal regulation to avoid bad behavior when the robot operates under higher level disturbances. This robust control problem will be solved in our next research works.

REFERENCES

[1]. Eloise Matheson, Riccardo Minto, Emanuele G. G. Zampieri, Maurizio Faccio and Giulio Rosati, Human–Robot Collaboration in Manufacturing Applications: A Review, *MDPI Robotics*, 2019, Vol 8, Issue 100, pp. 4-25.

[2]. Michael Shneier, Roger Bostelma, Literature Review of Mobile Robot, for Manufacturing, Intelligent Systems *Division Engineering Laboratory National Institute of Standards and Technology: US Department of Commerce*, NISTIR 8022M, May 2015,. pp. 5-21.

[3]. Francisco Rubio, Francisco Valero and Carlos Llopis-Alber, *A review of mobile robots: Concepts, methods, theoretical framework, and applications, International Journal of Advanced Robotic, Systems*, March-April 2019, pp. 1–22.

[4]. MARY B. ALATISE; GERHARD P. HANCKE, *A Review on Challenges of Autonomous Mobile Robot and Sensor Fusion Method*, IEEE Acces, VOL. 8, MARCH 2020, PP. 39830-39846.

[5]. Bai Rui, Kang Rongjie, Shang Kun, Yan Chenghao, Tang Zhao, Wand Ruiquin and Dai Jian, A humanoid robotic hand capable of internal assembly and measurement in spacesuit gloves, *Industrial Robots: An International Journal*, Vol. 49, No 4, February , pp. 603-615.

[6]. Swagat Chutia, Nayan M. Kakoty, Dhanapati Deka, *A Review of Underwater Robotics, Navigation, Sensing Techniques and Applications, conference on the advances robotics , navigation, sensing navigation and applications*, June 28-July 2, 2017, Nex Delhi, © Association for Computing Machinery.

[7]. T. Hellstrom, On the moral responsibility of military robots, *Information technology*, June 2013, volume 15 (issue 2), pp. 99 -107.

[8]. Lambèr Royakkers 1 · Rinie van Est, Int J of Soc Robotics (2015) 7:549–570, A Literature Review on New Robotics: Automation from Love to War, International Journal of Social Robotics, 2015; Vol. 7, pp. 549–570.

[9]. Manja Lohse, Frank Hegel, and Britta Wrede, Domestic Applications for Social Robot : An online survey on the influence of Appearance and capabilities, *Journal of Physical Agents, Vol. 2, no. 2*, June 2008, pp. 21-32.

[10]. MASAHIRO TAKENO, AKIRA MATSUMURA, SHIGERU SAKAMOTO, YOSHIHITO SAKAI, ATSUSHI SHIRATO, painting robot for exterior walls of high rise buildings, 1988 proceedings of the 5th isarc, tokyo, japan, ©1984-2022 THE INTERNATIONAL ASSOCIATION FOR AUTOMATION AND ROBOTICS IN CONSTRUCTION (IAARC).

[11]. Masahiro Takeno, Painting Robot for exterior walls of high rise buildings, *The 5th ISRO International symposium on robotics in constructions*, June 6-8, 1988, pp. 411-420, Tokyo, Japan.

[12]. Ryan A. Beasley, Medical Robots: Current Systems and Research Direction, *Journal of Robotics*, © Hindawi Publishing Corporation, Volume 2012, Article ID 401613, 14 pages.

[13]. Panagiotis Koustoumpardis, Paraskevi Zacharia, Nikos Aspragathos, Intelligent Robotic Handling of Fabrics towards Sewing, Chapter 28, in Book *Industrial Robotics: Programming, Simulation and Applications*, December 2006, pp. .559-582.

[14]. Maria Kyrarini, Fotios Lygerakis, Akilesh Rajavenkatanarayanan, Christos Sevastopoulos, Harish Ram Nambiappan , Kodur Krishna Chaitanya, Ashwin Ramesh Babu, Joanne Mathew and Fillia Make, A Survey of Robots in Healthcare, *MDPI Technologies*, January 2021, vol 9, no 8, 26 pages.

[15]. Michaud, F., Laplante, J. F., Larouche, H., Duquette, A., Caron, S., Létourneau, D., & Masson, P. (2005). Autonomous spherical mobile robot for child-development studies. *IEEE Transactions on Systems, Man and Cybernetics, Part A: Systems and Humans*, Vol 35, No 4, pp. 471-480.

[16]. Ruiz-del-Solar, J., & Avilés, R. (2004). Robotics courses for children as a motivation tool: The Chilean experience. *IEEE Transactions on Education*, 47(4), 474-480.

[17]. Mubin, O., Stevens, CJ., Shahid, S., Al Mahmud, A., & Dong, J. J. A Review of the applicability

of robots in education, *Technology for Education and Learning*, Vol 1, 2013, pp. 1-7.

[18]. Farhan A. Salem, Kinematics and Dynamic Models and Control for Differential Drive Mobile Robots *International Journal of Current Engineering and Technology,* Vol.3, No.2, June 2013, pp. 253-263.

[19]. Jakub CˇERKALA, Anna JADLOVSKÁ, Methodology for the Modelling of Mobile Robot with Differential Chassis, 16*th Scientific Conference of Young Researchers*, 01 June 2016, Košice (Slovak Republic),.

[20]. Mert Onkol, Cosku Kasnakoglu, Modeling and Control of a Robot Arm on a Two Wheeled Moving Platform, *Transactions Tech Publications of Switzerland: Applied Mechanics and Materials, Vols 789-790,* 2015, *pp. 735-741*.

[21]. Markov Djoumessi MBIHI, Bertrand Lonla MOFFO, Léandre NNEME NNEME, Dynamic and Kinematic Modelling with Virtual Simulation of Optimal PID/LQR Control Systems Based on Particle Swarm Optimization for 2WD Mobile Robots, Vol. 6, Issue 2, June-2021, pp. 89-110.

[22]. Loga Nga Fouda Jeanne, Kom Charles-Hubert, Moffo L. Bertrand, Jean Mbihi , "Implementation of a decoupled Digital feedback Control Architecture on an Arduino - Free RTOS Real Time Embedded System for Input Delay Robotic Servomechanism." International Review of Automatic Control, Vol 14, No 4, pp. 201-213, July 2021.

[23]. Hossein Sadegh Lafmejani, Hassan Zarabadipour, Modeling, Simulation and Position Control of 3DOF Articulated Manipulator, *Indonesian Journal of Electrical Engineering and Informatics*, Vol. 2, No. 3, September 2014, pp. 132-140.

[24]. Cherry Myint, Nu Nu Win, Position and Velocity control for Two-Wheel Differential Drive Mobile Robot, *International Journal of Science, Engineering and Technology Research,* Volume 5, Issue 9, September 2016, pp. 2845-2855.

[25]. Mert Onkol1,a, Cosku Kasnakoglu, Modeling and Control of a Robot Arm on a Two Wheeled Moving Platform, *Applied Mechanics and Materials Vols. 789-790,* 2015, *pp 735-741*

[26]. Mohd Ashiq Kamaril Yusoff, Reza Ezuan Saminb, Babul Salam Kader Ibrahim, Wireless Mobile Robotic Arm, *International Symposium on Robotics and Intelligent Sensors*, Procedia Engineering No 41, pp. 1072 – 1078, IRIS 2012.

[27]. P.Thompson, M. Rombaut, G. Rabatel, F. Pierrot, A. Liegeois, F. Sevila, "Design and Control of a Mobile Manipulator for Weed Control," Proc. of the Int. Conf. on Advanced Robotics, 1995, pp. 933-938.

[28]. M. H. Korayem, H. Ghariblu, "Maximum Allowable Load on Wheeled Mobile Manipulators Imposing Redundancy Constraints," Robotics and Autonomous Systems, vol. 44, 2003, pp. 151-159.

[29]. T. Sugar, V. Kumar, "Decentralized Control of Cooperating Mobile Manipulators," Proc. of the IEEE Int. Conf. on Robotics and Automation, Leuven, Belgium, 1998, pp. 2916-2921.

[30]. A. Leopoldo, MeARM UPV Quick Start laser cutting. Universitat Politecnica de Valencia, Jan. 2021.

[31]. J. Mbihi, "Experimental Modeling Approach of Dynamic Processes," in Analog Automation and Digital Feedback Control Techniques, ISTE and W., London: ISTE and John Wiley&Sons.

[32]. Y. Naung, A. Schagin, H. L. Oo, K. Z. Ye, and Z. M. Khaing, Implementation of data driven control system of DC motor by using system identification process, in 2018 IEEE Conference of Russian Young Researchers in Electrical and Electronic Engineering (EIConRus), Jan. 2018, pp. 1801–1804.